Current Opinion in Colloid & Interface Science 20 (2015) 11–18

Contents lists available at ScienceDirect

Current Opinion in Colloid & Interface Science

journal homepage: www.elsevier.com/locate/cocis

Depletion forces in thin liquid films due to nonionic and ionic surfactant micelles

Peter A. Kralchevsky, Krassimir D. Danov *, Svetoslav E. Anachkov

Department of Chemical & Pharmaceutical Engineering, Faculty of Chemistry and Pharmacy, Sofia University, Sofia 1164, Bulgaria

ARTICLE INFO

Article history:
Received 3 November 2014
Accepted 25 November 2014
Available online 4 December 2014

Keywords:
Depletion force
Oscillatory structural force
Nonionic micelles
Charged particles
Foam and emulsion films
Contact angles

ABSTRACT

The depletion force can be considered as a special (limiting) case of the oscillatory structural force at short distances between two surfaces. Here, we consider analytical expressions for the structural force in the depletion zone and compare their predictions with experimental data. In the case of particles that interact as hard spheres, an expression for the depth of the depletion minimum as a function of the particle volume fraction ϕ is available. This expression has been used to predict the rise of the contact angle α of plane-parallel foam films from nonionic surfactant solutions with the increase of surfactant concentration — a depletion effect due to the nonionic micelles, which can be treated as hard spheres. Further, knowing the theoretical α-vs.-ϕ dependence, from the experimental values of α the micelle aggregation number has been calculated, and the results agree well with data obtained by other methods. In the case of electrically charged particles, the depletion effect is strongly affected by the soft and long-range electrostatic repulsion. This interplay of electrostatic and depletion effects can be quantified by upgrading the Poisson–Boltzmann theory of electric double layer to take into account the presence of charged particles (macroions). The resulting theoretical model predicts the equilibrium thickness, h_0, of plane-parallel films formed from micellar solutions of ionic surfactants in excellent agreement with the experiment.

© 2014 Elsevier Ltd. All rights reserved.

1. Introduction

One of the first observations of depletion effect was reported by Bondy [1], who detected coagulation of rubber latex in the presence of polymer molecules in the disperse medium. Asakura and Oosawa [2] explained the observed interparticle attraction by the overlap of depletion layers at the surfaces of two neighboring colloidal particles. de Hek and Vrij [3] studied systematically the flocculation of sterically stabilized silica suspensions in cyclohexane by polystyrene molecules. Patel and Russel [4] investigated the phase separation and rheology of aqueous polystyrene latex suspensions in the presence of polymer (Dextran T-500). It was found [5] that in some cases the stability of dispersions is due to the balance between electrostatic repulsion and depletion attraction. Interplay of steric repulsion and depletion attraction was studied theoretically by van Lent et al. [6] for the case of polymer solution between two surfaces coated with anchored polymer layers. Joanny et al. [7] and Russel et al. [8] re-examined the theory of depletion interaction by taking into account the internal degrees of freedom of the polymer molecules. Their analysis confirmed the earlier results of Asakura and Oosawa [2]. Evans and Needham [9] measured the depletion energy of two interacting bilayer surfaces in a concentrated Dextran solution and their results also confirmed the basic paper, Ref. [2]. The effect of polymer polydispersity on the depletion interaction between two plates immersed in a nonadsorbing polymer solution was studied by the self-consistent-field theory [10]. The results showed that the range of the depletion potential increases, whereas the depth of the potential decreases with the rise of polydispersity. Synergistic effects of polymers and surfactants on the depletion forces have been also examined [11].

Depletion force in a bidisperse granular layer was investigated in experiments and simulations of mixtures of large and small steel spheres [12]. Sphere/wall and sphere/sphere interactions in a dilute suspension of infinitely thin rods were numerically calculated [13]. Shear-affected depletion interactions with disc-shaped particles were experimentally studied [14]. A detailed review on depletion surface forces can be found in the book by Lekkerkerker and Tuinier [15].

Foams and emulsions are often formed from solutions which contain colloidal particles. Such are the micellar solutions of nonionic and ionic surfactants, where the micelles play the role, respectively, of hard and charged spheres. In general, the confinement of colloid particles and surfactant micelles in liquid films gives rise to the oscillatory structural surface force [16,17]. The depletion interaction corresponds to the first minimum of the oscillatory force at small thicknesses, at which the particles are forced out of the film [18,19].

Based on the fact that the depletion force represents a special case of the oscillatory force, here we consider theoretical expressions for the oscillatory force in the depletion limit and compare their predictions with experimental data for the equilibrium thickness and contact angle of thin foam films formed from micellar surfactant solutions. In

* Corresponding author. Tel.: +359 2 8161396; fax: +359 2 9625643.
E-mail address: kd@lcpe.uni-sofia.bg (K.D. Danov).

http://dx.doi.org/10.1016/j.cocis.2014.11.010
1359-0294/© 2014 Elsevier Ltd. All rights reserved.

particular, Section 2 is dedicated to the case of particles that interact as hard spheres, which is an adequate model for uncharged colloidal beads and nonionic surfactant micelles. The cases of plane-parallel films (Fig. 1a) and two interacting larger particles (Fig. 1b) are considered. The available analytical expressions are compared with data for foam films from micellar solutions of nonionic surfactants. Likewise, in Section 3 we present analytical expressions describing electrostatic interactions influenced by the depletion force in the case of electrically charged particles. Next, the theoretical predictions are compared with the experimental equilibrium thicknesses of foam films formed from micellar solutions of ionic surfactants. The developed methodology can be applied to quantitatively interpret experimental data in many other systems affected by the depletion surface force.

2. Depletion attraction due to hard spheres and nonionic micelles

2.1. The depletion force as a special case of the oscillatory structural force

The stepwise thinning (stratification) of liquid films formed from solutions containing surfactant micelles or colloidal (e.g. latex) particles was interpreted as a layer-by-layer thinning of an ordered structure of micelles or particles inside the films [17,20,21], i.e. with the action of the oscillatory structural force [16,18,22–24]. At the final stage of film thinning, all micelles/particles are forced out of the film (Fig. 1a). Then, the two film surfaces experience a depletion attraction due to the osmotic pressure of the particles in the bulk liquid phase (Plateau border) around the film. In stable films, a repulsive force (electrostatic, steric, etc.) counterbalances the depletion attraction between the film surfaces. The depletion attraction affects the values of the final film thickness, h, and contact angle, α (Fig. 1a) — it tends to decrease h and increase α [25].

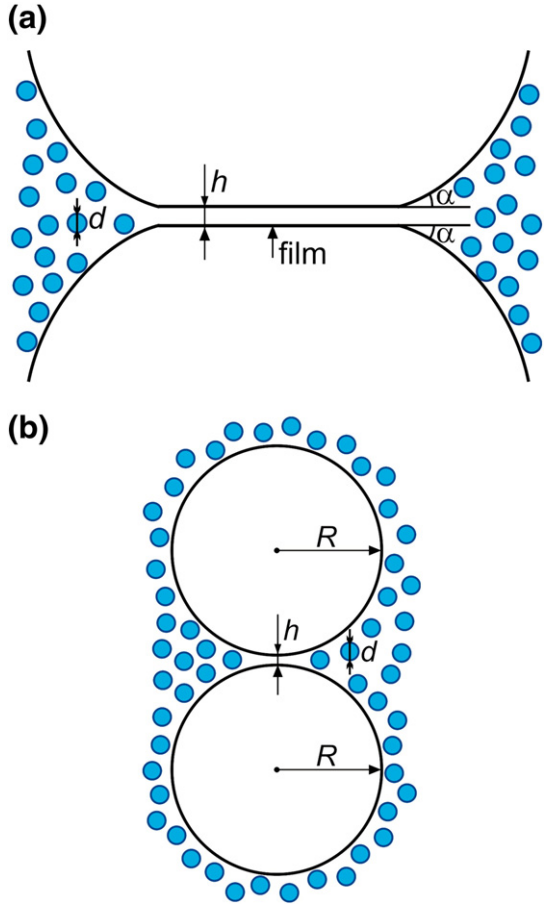

Fig. 1. (a) Sketch of a liquid film of thickness h, which is formed from a solution that contains uncharged colloidal spheres of diameter d; at $h < d$ the film does not contain any particles. (b) The depletion zone between two larger particles of radius R is the region of contact, where the smaller colloidal spheres cannot penetrate.

As already mentioned, the depletion force is a special case of the oscillatory structural force for $0 < h/d < 1$, where h is the thickness of the film's liquid core and d is the diameter of the particles that create the osmotic pressure. In superposition with the van der Waals and electrostatic surface forces, the depletion force gives rise to a minimum in the total interaction energy per unit area W at $h/d < 1$, which can be directly detected by colloidal probe atomic force microscopy (CP-AFM) [26], as well as by a surface-force apparatus [27]. In experiments with stratifying films, the effect of depletion interaction on the final film thickness, contact angle and disjoining pressure can be registered by using the capillary cell of Scheludko and Exerowa (SE cell) [28] and the porous-plate cell by Mysels and Jones (MJ cell) [29]; for examples, see Refs. [25,30]. At low values of the particle volume fraction ϕ, the oscillatory maxima and minima disappear, and the oscillatory structural force completely degenerates into the depletion force; see Fig. 2a.

2.2. Quantitative theoretical description for hard spheres

In the case of particles and micelles that can be treated as hard spheres, the oscillatory structural force (and the depletion force as its special case) has been calculated by using the equations of statistical mechanics [24,31–33] and numerical simulations [19,34,35]. Simpler, but quantitative semiempirical expressions have been proposed [18,36] on the basis of analytical and numerical results for hard sphere fluids. Here, following Ref. [25] we will present the predictions and application of the model from Ref. [36], which has been successfully tested against data from Monte Carlo simulations, CP-AFM measurements [37] and data for stratifying films [25]. This model yields the following expressions for the interaction energy per unit area of a plane-parallel film due to the oscillatory force, W_{osc} [36]:

$$\frac{W_{osc}d^2}{kT} = -\frac{p_{hs}d^3}{kT}\left(1-\hat{h}\right) - \frac{2\sigma_{hs}d^2}{kT}, \quad \text{for } 0 \le \hat{h} < 1 \tag{1}$$

$$\frac{W_{osc}d^2}{kT} = w_0 \cos\left(\omega\hat{h} + \varphi_1\right) e^{-q\hat{h}} + w_1 e^{\delta(1-\hat{h})}, \quad \text{for } \hat{h} \ge 1. \tag{2}$$

Here, $\hat{h} = h/d$ is the dimensionless surface-to-surface distance; d is the micelle diameter; k is the Boltzmann constant and T is the absolute temperature; p_{hs} is the pressure of a hard-sphere fluid expressed through the Carnahan–Starling formula [38], and σ_{hs} is the scaled-particle-theory [39] expression for the excess surface free energy of a hard-sphere fluid:

$$\frac{p_{hs}d^3}{kT} = \frac{6}{\pi}\phi\frac{1+\phi+\phi^2-\phi^3}{(1-\phi)^3} \tag{3}$$

$$\frac{\sigma_{hs}d^2}{kT} = -\frac{9}{2\pi}\phi^2\frac{1+\phi}{(1-\phi)^3}. \tag{4}$$

The parameters w_0, ω, φ_1, q, w_1 and δ in Eq. (2) are known functions of the hard-sphere (micelle) volume fraction, ϕ; see, e.g., Eqs. (8)–(16) in Ref. [37]. In particular, the parameters w_0, ω, and q characterize, respectively, the amplitude, period and decay length of the oscillations.

Fig. 2a shows the dependence of the dimensionless energy $W_{osc}d^2/(kT)$ on h/d calculated from Eqs. (1)–(4) for three different particle volume fractions, $\phi = 0.15$, 0.26 and 0.38. At the lowest volume fraction, $\phi = 0.15$, the amplitude of the oscillatory maxima and minima is rather small and the interaction energy is dominated by the *depletion minimum* at $h/d < 1$. At the greater values of ϕ, the amplitude of decaying oscillations at $h/d > 1$ increases considerably, and the depletion minimum of W_{osc} becomes deeper.

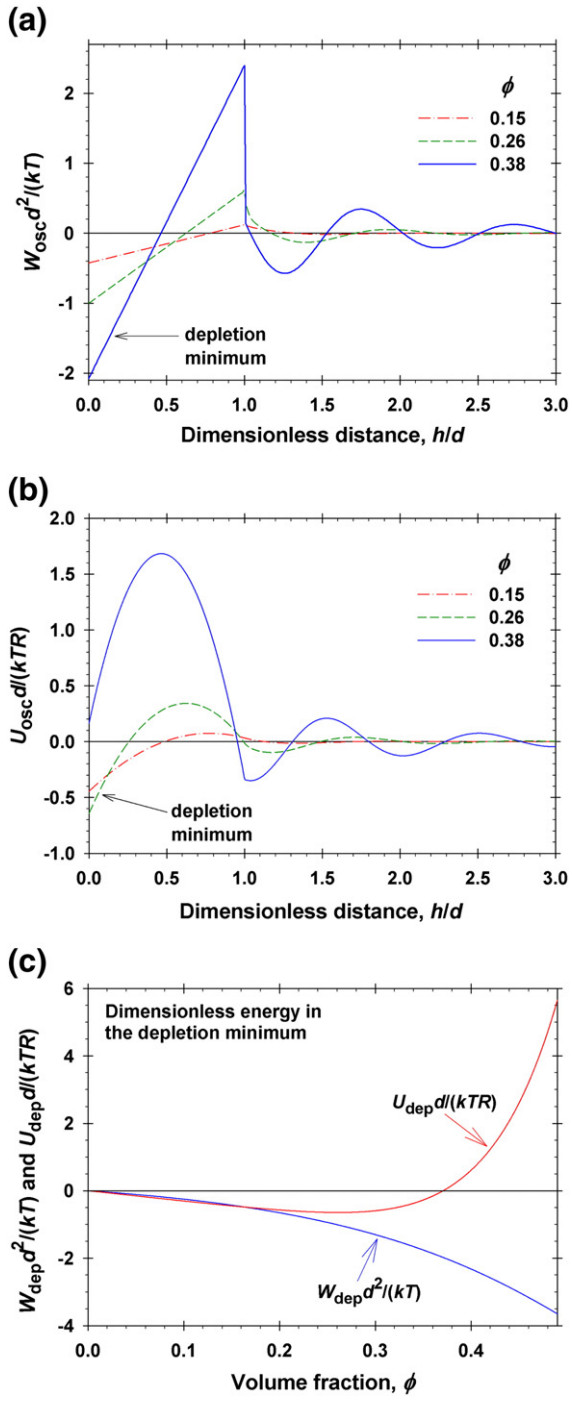

Fig. 2. (a) Plot of the dimensionless energy of the oscillatory structural force per unit area of the film, $W_{osc}d^2/(kT)$, calculated from Eqs. (1)–(4), vs. the dimensionless film thickness h/d. (b) Plot of the dimensionless energy of interaction between two particles, $U_{osc}d/(kTR)$ vs. h/d, calculated from Eq. (5). (c) Comparison of the dependencies of W_{dep} and U_{dep} on the volume fraction ϕ of the small particles.

The contribution of the oscillatory structural force to the energy (U_{osc}) of interaction between two colloidal spheres, which are immersed in a fluid of smaller colloidal spheres of diameter d (Fig. 1b), can be calculated by integrating $W_{osc}(h,\phi)$ in accordance with the Derjaguin's approximation [40]:

$$U_{osc}(h,\phi) = \pi R \int_h^\infty W_{osc}\left(\bar{h},\phi\right) d\bar{h}. \tag{5}$$

Here, h is the shortest surface-to-surface distance between the two spheres of radius R and $\bar{h}$ is an integration variable. The substitution of W_{osc} from Eqs. (1) and (2) into Eq. (5) leads to an analytical expression for $U_{osc}(h,\phi)$ (see Ref. [25]), which has been used to calculate the curves in Fig. 2b. In particular, the depth of the depletion minimum, $U_{dep} = U_{osc}(0,\phi)$, is given by the expression:

$$\frac{U_{dep}(\phi)d}{kTR} = -\frac{\pi d^2}{2kT}(p_{hs}d + 4\sigma_{hs}) + u_{osc}(1,\phi) \tag{6}$$

where p_{hs} and σ_{hs} are given by Eqs. (3) and (4), and

$$u_{osc}(1,\phi) = \frac{\pi w_0 e^{-q}}{\omega^2 + q^2}[q\cos(\omega+\varphi_1) - \omega\sin(\omega+\varphi_1)]. \tag{7}$$

Note that the configurations shown in Fig. 1a and b correspond to interactions described by Eqs. (1)–(2) and (5)–(6), respectively.

As illustrated in Fig. 2b, the amplitude of the oscillations markedly increases with the rise of ϕ, the first maximum always having the greatest amplitude. At lower ϕ, the depletion minimum, $U_{dep} = U_{osc}(0,\phi)$, is the deepest one as compared with the oscillatory minima at greater h values. At $\phi = 0.26$, its depth (characterized by the algebraic value of U_{dep}) is the maximal: $U_{dep}d/(kTR) = -0.64$. For $\phi > 0.26$, U_{dep} increases, and for $\phi > 0.37$ it becomes positive. Nevertheless, the depletion minimum always leads to particle aggregation because the first oscillatory maximum serves as a high barrier to particle detachment.

In Fig. 2c, the non-monotonic dependence U_{dep} vs. ϕ is compared with the monotonic dependence of $W_{dep} \equiv W_{osc}(0,\phi)$ on ϕ. At close contact between the two surfaces (for a thin film without particles/micelles), the depth of the depletion minimum, $|W_{dep}(\phi)|$, is an increasing function of ϕ, in agreement with the experiment [26]. Physically, this means that the depletion attraction (due to the sucking osmotic pressure engendered by the particles in the bulk phase) increases with the rise of ϕ. In contrast, because $U_{dep}(\phi)$ is an integral of $W_{osc}(h,\phi)$, see Eq. (5), it contains contributions not only from the depletion zone ($0 < h/d < 1$), but also from the oscillatory zone ($h/d > 1$), thus including zones of negative and positive W_{osc}. Physically, this is due to the fact that the gap between two spherical particles (Fig. 1b) has a non-uniform thickness, where the local excess pressure could be either attractive or repulsive depending on the local thickness. For this reason, it is not obvious whether the attraction or repulsion will prevail in the integral interaction energy between two spherical particles in contact, $U_{dep}(\phi)$. Fig. 2b shows that both cases ($U_{dep} < 0$ and $U_{dep} > 0$) are possible depending on the value of ϕ [25]. The non-monotonic behavior of the depletion-minimum depth $U_{dep}(\phi)$ predicted by the semiempirical model, Eqs. (1)–(4), needs to be validated by independent methods, e.g. computer simulations.

The applicability of the Derjaguin approximation to calculate depletion forces is sometimes called into question. To clarify this point, here we briefly recall the derivation of the Derjaguin's formula and the used approximations. After White [41], we consider the general case of two curved (not necessarily spherical) surfaces. The goal is to calculate the energy of interaction, $U(h)$, between two curved surfaces (e.g. the two particles in Fig. 1b) using the expression for the interaction energy per unit area of a plane-parallel film, $W(h)$. The latter is the work to bring the two film surfaces from infinity to a finite separation h. Derjaguin proposed the formula [40,42]:

$$U = \int_{-\infty}^{\infty}\int_{-\infty}^{\infty} W(h(x,y))\,dx\,dy \tag{8}$$

$h(x,y)$ is the running distance between the two curved surfaces in the contact zone; the integration is carried out over the midplane between the two particles, and (x,y) are Cartesian coordinates in the midplane. The energy $W(h)$ must decay sufficiently rapidly with distance h so

that contributions to U are insignificant from area elements very far from the zone of close contact. Furthermore, using the fact that the two smooth curved surfaces can be approximated by paraboloids in the contact zone, $h(x,y)$ can be expressed in the form [41–43]:

$$h = h_0 + \frac{1}{2}c\,x^2 + \frac{1}{2}c'\,y^2 \tag{9}$$

where c and c' are coefficients depending on the surface geometry in the contact zone. Next, polar coordinates (ρ,φ) are introduced in the xy-plane:

$$x = \frac{\rho}{\sqrt{c}}\cos\varphi, \quad y = \frac{\rho}{\sqrt{c'}}\sin\varphi. \tag{10}$$

Then, Eq. (8) acquires the form:

$$U = \int_0^{2\pi}\int_0^{\infty} W(h(\rho))\frac{\rho d\rho d\varphi}{\sqrt{cc'}} \tag{11}$$

where $h = h_0 + \frac{1}{2}\rho^2$ (the dimension of ρ is $m^{1/2}$). Integrating with respect to φ and using the relationship $dh = \rho\, d\rho$ one finally obtains [41]:

$$U(h_0) = \frac{2\pi}{\sqrt{cc'}}\int_{h_0}^{\infty} W(h)dh, \qquad \text{(interaction energy)}. \tag{12}$$

Mathematically, one can derive [41–43]

$$cc' = c_1c_1' + c_2c_2' + (c_1c_2 + c_1'c_2')\sin^2\omega + (c_1c_2' + c_1'c_2)\cos^2\omega. \tag{13}$$

Here, c_1 and c_1' are the principal curvatures of the first surface, whereas c_2 and c_2' are the principal curvatures of the second surface in the contact zone; ω is the angle subtended between the directions of the principle curvatures of the two surfaces in this zone. It was confirmed both theoretically [32] and experimentally [44] that Eq. (12) provides a good approximation for the interaction energy in the range of its validity.

For two spherical particles of radius R separated at a surface-to-surface distance h_0 (Fig. 1b) one has $c_1 = c_1' = c_2 = c_2' = 1/R$. Then, from Eqs. (12) and (13) we obtain Eq. (5).

For two crossed cylinders used in the surface force apparatus [16], i.e. for two infinitely long rods of radii r_1 and r_2 separated at a transversal surface-to-surface distance h_0 and subtending an angle ω, one has $c_1 = 1/r_1$, $c_1' = 0$, $c_2 = 1/r_2$ and $c_2' = 0$. Then, Eqs. (12) and (13) lead to

$$U(h_0) = \frac{2\pi\sqrt{r_1r_2}}{\sin\omega}\int_{h_0}^{\infty} W(h)dh \qquad \text{(two cylinders)}. \tag{14}$$

Because of the general mechanical (phenomenological) approach used for its derivation, the generalized Derjaguin's formula, Eq. (12), is applicable to any type of force law (attractive, repulsive, oscillatory) if only (i) the range of the forces and (ii) the surface-to-surface distance are much smaller than the surface curvature radii [41]. This formula is applicable to any kind of surface force, irrespective of its physical origin: van der Waals, electrostatic, steric, oscillatory-structural, depletion, etc.

2.3. Effect of depletion forces on the contact angles of foam films

As an illustrative example for the application of the above theoretical model, let us consider a foam film formed from a micellar solution of nonionic surfactant. At the final stage of film thinning, no micelles are present in the film (Fig. 1a), but the osmotic effect of the micelles in the Plateau border gives rise to attraction between the film surfaces, which is counterbalanced by the steric repulsion between the two surfactant adsorption layers. Insofar as the steric repulsion can be modeled as hard wall repulsion, the contact angle α of the foam film (Fig. 1a) is determined by a superposition of the van der Waals and depletion attraction [25,45]:

$$\cos\alpha = 1 + \frac{W_{vw} + W_{dep}(\phi)}{2\sigma} \tag{15}$$

σ is the solution's surface tension; W_{vw} is the energy of van der Waals interaction per unit area of the film [16]:

$$W_{vw} = -\frac{A_H}{12\pi h_0^2} \tag{16}$$

h_0 is the final thickness of the film; A_H is the Hamaker constant; as before $W_{dep} = W_{osc}(0,\phi)$ is the energy of the depletion interaction per unit area of the film [25]:

$$W_{dep}(\phi) = -\frac{6kT}{\pi d^2}\frac{\phi}{(1-\phi)^3}\left(1 - \frac{\phi}{2} - \frac{\phi^2}{2} - \phi^3\right). \tag{17}$$

Eq. (17) follows from Eqs. (1), (3) and (4) for $h = 0$ and corresponds to the depletion minimum. In agreement with the experiments (see Table 1), Eqs. (15) and (17) indicate that the contact angle should increase with the rise of ϕ in the whole interval $0 \le \phi \le 0.494$. The upper limit $\phi = 0.494$ corresponds to the Kirkwood–Alder–Wainwright phase transition in a hard-sphere fluid [46,47]. For micelles of diameter d, the micelle volume fraction ϕ is related to the total surfactant concentration, C_s, and the micelle aggregation number, N_{agg}, by the equation [25]:

$$N_{agg} = \frac{\pi d^3}{6}\frac{C_s - \mathrm{CMC}}{\phi} \tag{18}$$

where CMC denotes the critical micellization concentration. From the experiment, we know C_s, CMC and d, whereas ϕ is unknown. In particular, d can be determined by dynamic light scattering, or estimated as the doubled length of the surfactant molecule. N_{agg} is expected to slightly increase with the rise of C_s [48].

Under such circumstances, the predictions of the model of depletion interaction can be verified in the following way. First, for given experimental values of the contact angle α and the final film thickness h_0, we calculate the micelle volume fraction, ϕ from Eqs. (15)–(17). Second, the determined ϕ is substituted in Eq. (18) and the obtained N_{agg} is compared with experimental data for the micelle aggregation number.

Table 1 shows data for α and h_0 measured by an SE cell for foam films from micellar solutions of the nonionic surfactants Brij 35 and Tween 20. Because h_0 is an equivalent water thickness of the film determined interferometrically [25,28,30], the value of the Hamaker constant for water, $A_H = 3.7 \times 10^{-20}$ J [16], is to be used in Eq. (16). The other parameter values are as follows: $d = 8.8$ nm and CMC $= 9 \times 10^{-5}$ M for Brij 35, and $d = 7.2$ nm and CMC $= 5 \times 10^{-5}$ M for Tween 20. The

Table 1
Experimental data from [25] for the final film thickness h_0 and contact angle α of films from micellar solutions of the nonionic surfactants Brij 35 and Tween 20, and calculated micelle bulk volume fraction ϕ and aggregation number N_{agg} (details in the text).

C_s (mM)	h_0 (nm)	α (deg)	ϕ	N_{agg}
Brij 35				
10	14	0.87	0.033	65
50	13	1.64	0.163	66
80	12.5	2.24	0.257	67
100	12	2.65	0.315	69
Tween 20				
80	10.4	1.87	0.135	70
100	10.2	2.09	0.167	70

last two columns of Table 1 show the values of ϕ and N_{agg} determined as explained in the previous paragraph. The obtained N_{agg} is in good agreement with literature data and molecular-size estimates; see Ref. [25] for details. These results confirm the adequacy of the described model of depletion attraction in a hard-sphere fluid.

3. Depletion attraction due to charged particles and micelles

3.1. Electrostatic interactions influenced by the depletion effect

Here, we consider the occurrence of the depletion effect with charged particles, including micelles of ionic surfactants. In this case, the hard-core repulsion is replaced with the soft and long-range electrostatic repulsion, which is acting between each two particles; between the particles and the film surface, and between the two surfaces of the liquid film. We are dealing with electrostatic interactions influenced by the depletion effect.

Fig. 3 represents a sketch of a liquid film formed from a solution containing charged particles. The two main differences with the case of uncharged particles are as follows. Firstly, the main contribution in the osmotic pressure is due to counterions dissociated from the charged particles (micelles), rather than to the particles themselves.

Secondly, because of the powerful repulsion between the two like-charged film surfaces, the final (equilibrium) film can be considerably thicker than the micelle diameter. For example, Fig. 4a shows data for the evolution of the thickness of foam films formed from micellar solutions of sodium dodecyl sulfate (SDS). The thickness undergoes stepwise transitions (stratification) due to the oscillatory structural force. The steps of thickness h_0, h_1 and h_2 correspond to states of the film in which it contains, respectively, $n = 0$, 1 and 2 layers of micelles. In particular, at 50 mM SDS the equilibrium thickness of the film is $h_0 =$ 17.3 nm, whereas the hydrodynamic diameter of the SDS micelle is 4.6 nm [49]. In such a case, the expulsion of the micelles from the film interior (the depletion effect) is due to the long-range electrostatic repulsion, rather than to the hard-core effect (as in Fig. 1a). Because the electrostatic repulsion is soft, some micelles can penetrate into the film (Fig. 3) driven by the entropy of mixing. However, at $h = h_0$ the micellar concentration in the film is much lower than that in the neighboring bulk liquid phase [49].

For $h < h_1$ (in the depletion zone) the disjoining pressure in the film can be presented in the form

$$\prod(h) = \prod_{el}(h) + \prod_{vw}(h) \tag{19}$$

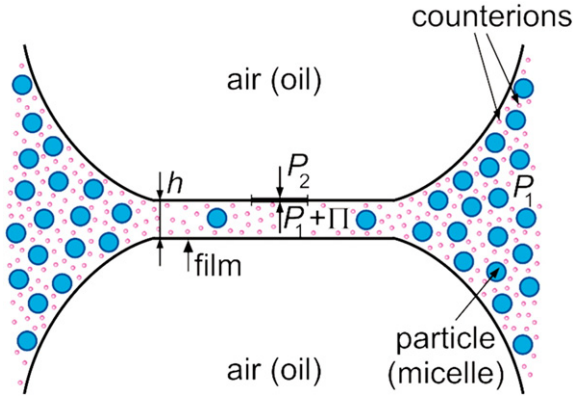

Fig. 3. Sketch of a liquid film of thickness h, which is formed from a solution containing charged colloidal particles (e.g. ionic surfactant micelles). The main particle contribution to the osmotic pressure is due to counterions (depicted as dots) dissociated from the particles. P_1 and P_2 are the pressures in the aqueous suspension and in the air (oil), whereas Π is the additional "disjoining" pressure acting per unit area of the film surface.

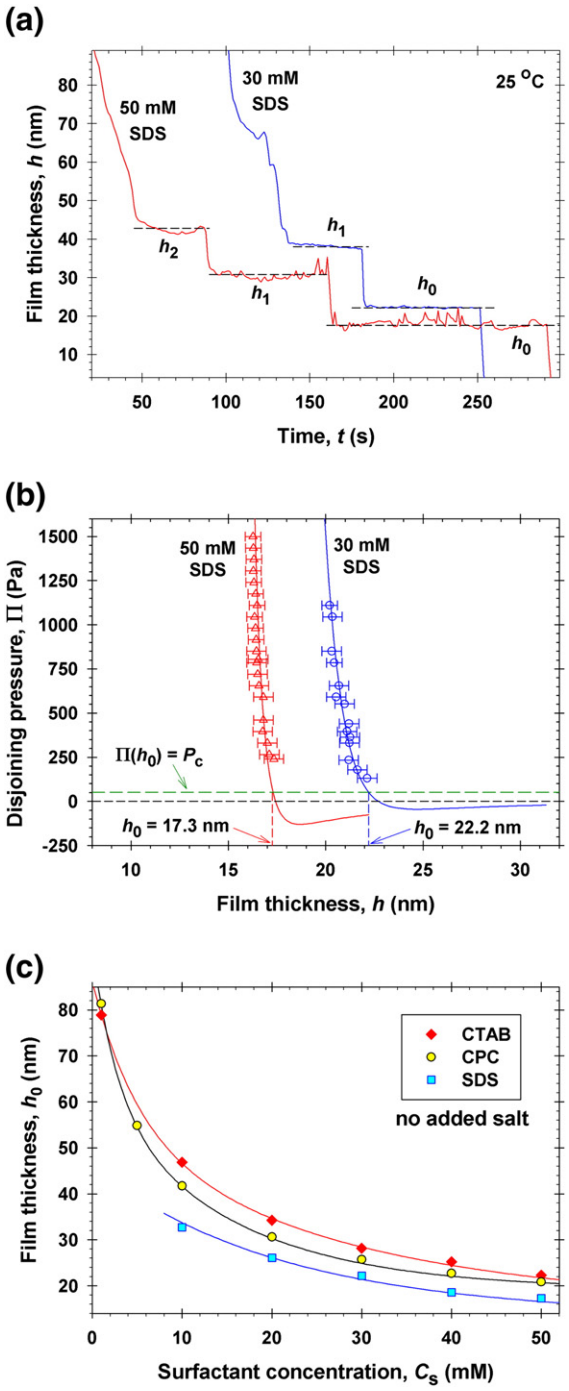

Fig. 4. (a) Experimental stepwise thinning of a foam film formed from a micellar SDS solution in an SE cell [49]. (b) Comparison of the calculated $\Pi(h)$ dependences in the depletion zone (the solid lines) with experimental data obtained by an MJ cell [50]; the equilibrium thickness h_0 is determined from the equation $\Pi(h_0) = P_c$. (c) Plots of h_0 vs. C_s; the points are experimental values; the solid lines are predicted by the theory without using any adjustable parameters [49]; details in the text.

where Π_{el} represents the contribution of the electrostatic interaction influenced by the depletion effect, whereas Π_{vw} is the van der Waals component of disjoining pressure:

$$\prod_{vw}(h) = -\frac{A_H}{6\pi h^3} \tag{20}$$

Π_{el} is equal to the difference between the osmotic pressures in the midplane of the film and in the bulk solution [16,49]:

$$\Pi_{el} = (P_{osm})_{midplane} - (P_{osm})_{bulk}. \quad (21)$$

The bulk osmotic pressure can be estimated from the expression [49]:

$$(P_{osm})_{bulk} = kT\left[2(c_1 + c_3) + (Z+1)c_p\right]. \quad (22)$$

The first term in the brackets in Eq. (22) expresses the contributions from the background electrolyte. In the case of micellar solution of an ionic surfactant, c_1 is the bulk concentration of surfactant monomers; c_3 is the bulk concentration of coions from the added electrolyte (if any), and the multiplier 2 stands for their counterions; 1:1 electrolytes are assumed. The second term in the brackets is the contribution of the particles/micelles (c_p) and of the counterions dissociated from them (Zc_p); Z is the number of elementary charges per particle/micelle. Likewise, the osmotic pressure in the middle of the film can be estimated using the Boltzmann law for the concentrations of ions in electric field [49]:

$$(P_{osm})_{midplane} = kT\left[(c_1 + c_3)\left(e^{\Phi_m} + e^{-\Phi_m}\right) + Zc_p e^{\Phi_m} + c_p e^{-Z\Phi_m}\right]. \quad (23)$$

Here, $\Phi_m = e|\psi_m|/(kT)$ is the dimensionless electric potential in the film midplane; ψ_m is the respective dimensional potential and e is the magnitude of the elementary electric charge. The contribution of the depletion effect to Π_{el} can be identified with the terms proportional to c_p in Eqs. (22) and (23).

As mentioned above, the predominant contribution of the charged particles to P_{osm} is due to counterions dissociated from their surfaces. The effect of the finite particle volume, which is important for uncharged particles, becomes negligible for charged particles. To demonstrate that, let us expand the fraction in Eq. (3) in series for small ϕ. The second term in this expansion, $4kTc_p\phi$ where $c_p = 6\phi/(\pi d^3)$, gives the contribution of the finite particle volume to the osmotic pressure. On the other hand, the osmotic contribution of the "point" particles and their counterions to Eq. (22) is $(Z+1)kTc_p$. The ratio of these two terms, $4\phi/(Z+1)$, is a small quantity. For example, using parameter values for SDS from Eq. (18) one estimates $\phi \approx 0.05$ for micelles of hydrodynamic diameter $d = 4.8$ nm and aggregation number $N_{agg} = 65$ in 100 mM SDS solution. With $Z = 35$, this yields $4\phi/(Z+1) = 5.6\times10^{-3}$, i.e. the osmotic effect of the micelle finite volume is really negligible as compared with the osmotic effect of the "point" particle and the dissociated counterions.

3.2. Comparison of theory and experiment

The theory of electrostatic interactions influenced by the depletion effect can be verified by comparing its predictions with the experimental dependence of the final thickness of foam films, h_0, on the total surfactant concentration, C_s, for micellar solutions of ionic surfactants [49]. Theoretically, h_0 can be determined as a solution of the equation

$$\Pi(h_0) = P_c \quad (24)$$

where Π is given by Eqs. (19)–(23) and P_c is a constant parameter — the capillary pressure, which is known from the experiment. The Laplace pressure of the curved meniscus is $P_c = P_2 - P_1$, where P_2 and P_1 are the pressures in the air (oil) and in the aqueous suspension; see Fig. 3. As illustrated in this figure, the force balance per unit area of the film surface reads $P_2 = P_1 + \Pi$, which is equivalent to Eq. (24).

In view of Eq. (23), to find the dependence $\Pi(h_0)$, we have to determine the dependence $\Phi_m(h)$. For that purpose, we have to integrate the Poisson–Boltzmann equation, which can be presented in the form:

$$\frac{d^2\Phi}{dx^2} = 4\pi L_B\left[2(c_1 + c_3)\sinh\Phi + Zc_p\left(e^{\Phi} - e^{-Z\Phi}\right)\right]. \quad (25)$$

The x-axis is perpendicular to the film surfaces and $x = 0$ corresponds to the film midplane; $\Phi = e|\psi|/(kT)$ is the dimensionless electric potential; ψ is the respective dimensional potential; $L_B = e^2/(4\pi\varepsilon\varepsilon_0 kT)$ is the Bjerrum length, which is equal to 0.72 nm for water at 25 °C. From Eq. (25), using two subsequent integrations one can derive [49,50]:

$$(2\pi L_B)^{1/2}\tilde{h} = \int_{\Phi_m}^{\Phi_s} [F(\Phi, \Phi_m)]^{-1/2} d\Phi \quad (26)$$

$$F(\Phi, \Phi_m) = 2(c_1 + c_3)(\cosh\Phi - \cosh\Phi_m) + Zc_p\left(e^{\Phi} - e^{\Phi_m}\right) + c_p\left(e^{-Z\Phi} - e^{-Z\Phi_m}\right) \quad (27)$$

where $\tilde{h} = h - h_a$ is the thickness of the aqueous core of the film; h is the total film thickness, including the two surfactant adsorption layers, each of them of thickness $h_a/2$; Φ_s is the dimensionless electrostatic potential at the film surface; Φ_s can be determined from the first integral of the Poisson–Boltzmann equation [49,50]:

$$\frac{\Gamma_1}{1 + K_{St}\gamma_{\pm}c_2\exp\Phi_s} = \left[\frac{1}{2\pi L_B}F(\Phi_s, \Phi_m)\right]^{1/2}. \quad (28)$$

Γ_1 is the adsorption (surface density) of surfactant molecules at the air/water interface; $c_2 = c_1 + c_3 + Zc_p$ is the bulk concentration of free counterions. The left-hand side of Eq. (28) represents the film surface charge density expressed through the Stern equation of counterion binding, whereas the right-hand side of Eq. (28) represents the same quantity expressed through the Gouy equation for the film, which relates the surface charge with the surface potential; $\gamma_{\pm}$ is the activity coefficient; for details, see [49]. The term with K_{St} in Eq. (28) accounts for the effect of counterion binding at the film surface, which decreases the effective surface charge. The adsorption at CMC, $\Gamma_1 = 2.41\times10^{18}$ molecules/m^2 and the Stern constant, $K_{St} = 0.653$ M^{-1} have been determined from fits of surface-tension isotherms for SDS [49].

It is convenient to calculate the $\Pi_{el}(h)$ dependence in parametric form: $\Pi_{el} = \Pi_{el}(\Phi_m)$ and $h = h(\Phi_m)$. For known c_1, c_3, c_p, and Z ($Z \approx 35$ for SDS micelles), and for a given Φ_m, we calculate $\Pi_{el}(\Phi_m)$ from Eqs. (21)–(23). Next, from Eqs. (26) and (27) we calculate the dependence $h(\Phi_m)$, where Φ_s is determined from Eq. (28). Furthermore, $\Pi = \Pi_{el} + \Pi_{wv}$ is calculated using Eq. (20). By variation of Φ_m, we find the value of this quantity, for which $\Pi = P_c$, i.e. Eq. (24) is satisfied. The respective value of $h = h_0$ is the equilibrium film thickness.

As an illustration, in Fig. 4b we compare the theoretical disjoining pressure isotherm $\Pi(h)$ in the depletion zone, calculated as described above, with the experimental $\Pi(h)$ isotherm independently measured by means of an MJ cell at two SDS concentrations, $C_s = 30$ and 50 mM [50]. The theoretical curves agree very well with the experiment; no adjustable parameters have been used. In accordance with Eq. (24), the intersection points of the horizontal line $\Pi = P_c = $ const. with the $\Pi(h)$ curves determines the equilibrium film thickness, h_0. For the considered experiments, the capillary pressure value is $P_c = 52$ Pa [50].

In this way, one can calculate h_0 for various total surfactant concentrations, C_s. As seen in Fig. 4c, the theoretical h_0 vs. C_s dependencies are in excellent agreement with experimental data for three surfactants: SDS, CTAB (cetyl trimethylammonium bromide) and CPC (cetylpyridinium chloride); no adjustable parameters have been used.

The excellent agreement between theory and experiment can be utilized to solve the reverse problem, viz. to determine the micelle charge Z

from the measured final film thickness, h_0. This approach has been used in Ref. [50] to find the values of Z at various concentrations of six different surfactants. Furthermore, one can determine the degree of micelle ionization, $\alpha_{mic} = Z/N_{agg}$. For ionic surfactants, the aggregation number N_{agg} can be calculated from the height of the step, Δh, determined in the same film-stratification experiment, as in Fig. 4a:

$$N_{agg} = (C_s - \mathrm{CMC})(\Delta h)^3. \quad (29)$$

In Eq. (29), C_s and CMC have to be expressed as number of molecules per unit volume. The values of N_{agg} determined from Eq. (29) are in very good agreement with aggregation numbers determined by other methods; see Refs. [30,49,50] for details.

The above quantitative approach can be used to determine the disjoining pressure $\Pi(h)$ and film thickness h in the depletion zone, $0 < h < h_1$. Unfortunately, in the case of electrically charged particles analytical theory for $\Pi(h)$ in the zone of the oscillatory structural force, $h \geq h_1$, has not yet been developed. For this reason, there are no analytical expressions for the energy per unit film area, $W(h)$, and the interaction energy between two particles, $U(h)$, which represent integrals of $\Pi(h)$ over the whole range of film thicknesses, including both the depletion and oscillatory zones. For $h \geq h_1$, only numerical results obtained by Monte Carlo simulations are available [51,52].

In the case of charged particles, the upper limit of the depletion zone, h_1, can be identified as the experimental thickness of the stratification step with one layer of micelles in the film; see Fig. 4a. Theoretically, this limit can be estimated as $h_1 = h_0 + d_{eff}$, where d_{eff} is the effective diameter of the charged micelle (particle) given by Eq. (3) in Ref. [50], and h_0 can be determined as described above.

4. Summary and conclusions

The confinement of colloidal particles between two surfaces gives rise to the oscillatory structural surface force. The depletion force represents a special (limiting) case of the structural force at short distances between the two surfaces. Here, we consider analytical expressions for the structural force in the depletion zone and compare their predictions with experimental data.

The analytical semiempirical model of structural force [36], which is based on the expressions by Carnahan–Starling [38] and scaled-particle theory [39] for hard sphere fluids, has been used to derive an expression for the depth of the depletion minimum, W_{dep}, as a function of the particle volume fraction, ϕ; see Eq. (17). This expression can be used to predict the rise of the contact angle, α, of plane-parallel foam films from nonionic surfactant solutions with the increase of surfactant concentration. The effect is due to the depletion effect of the nonionic surfactant micelles, which can be treated as hard spheres. Further, knowing the theoretical α-vs.-ϕ dependence, from the experimental values of α the micelle aggregation number, N_{agg}, was calculated. The results compare very well with values of N_{agg} obtained by other methods (see Table 1). In this way, the applicability of the considered model of the oscillatory structural force to calculate the depletion force is confirmed for the case of particles that interact as hard spheres.

In the case of electrically charged particles, the depletion effect is strongly affected by the soft and long-range electrostatic repulsion. In this case, the osmotic effect of the finite particle volume becomes negligible in comparison with the osmotic effect of the counterions dissociated from the particles. The interplay of electrostatic and depletion effects can be quantified by upgrading the Poisson–Boltzmann theory of electric double layer to take into account the presence of charged particles (macroions). The contribution of the depletion effect can be identified with the terms containing the particle concentration, c_p; see Eqs. (21)–(23). The resulting theoretical model predicts the equilibrium thickness, h_0, of plane-parallel foam films formed from micellar solutions of ionic surfactants in excellent agreement with the experiment (Fig. 4c). Further efforts are necessary to quantify the depletion effect for non-planar charged surfaces.

Acknowledgments

The authors gratefully acknowledge the support from the FP7 project Beyond-Everest, and from COST Action CM1101.

References

[1] Bondy C. The creaming of rubber latex. Trans Faraday Soc 1939;35:1093–108. http://dx.doi.org/10.1039/TF9393501093.
[2] Asakura S, Oosawa F. On interaction between two bodies immersed in a solution of macromolecules. J Chem Phys 1954;22:1255–6. http://dx.doi.org/10.1063/1.1740347.
[3] de Hek H, Vrij A. Interactions in mixtures of colloidal silica spheres and polystyrene molecules in cyclohexane: I. Phase separations. J Colloid Interface Sci 1981;84:409–22. http://dx.doi.org/10.1016/0021-9797(81)90232-0.
[4] Patel PD, Russel WB. An experimental study of aqueous suspensions containing dissolved polymer: A. Phase separation. J Colloid Interface Sci 1989;131:192–200. http://dx.doi.org/10.1016/0021-9797(89)90158-6.
[5] Aronson MP. The role of free surfactant in destabilizing oil-in-water emulsions. Langmuir 1989;5:494–501. http://dx.doi.org/10.1021/la00086a036.
[6] van Lent B, Israels R, Scheutjens JMHM, Fleer GJ. Interaction between hairy surfaces and the effect of free polymer. J Colloid Interface Sci 1990;137:380–94. http://dx.doi.org/10.1016/0021-9797(90)90414-J.
[7] Joanny JF, Leibler L, de Gennes PG. Effects of polymer solutions on colloid stability. J Polym Sci 1979;17:1073–84. http://dx.doi.org/10.1002/pol.1979.180170615.
[8] Russel WB, Saville DA, Schowalter WR. Colloidal dispersions. Cambridge: University Press; 1989.
[9] Evans E, Needham D. Attraction between lipid bilayer membranes in concentrated solutions of nonadsorbing polymers: comparison of mean-field theory with measurements of adhesion energy. Macromolecules 1988;21:1822–31. http://dx.doi.org/10.1021/ma00184a049.
[10] Yang S, Tan H, Yan D, Nies E, Shi A-C. Effect of polydispersity on the depletion interaction in nonadsorbing polymer solutions. Phys Rev E 2007;75:061803. http://dx.doi.org/10.1103/PhysRevE.75.061803.
[11] Tulpar A, Tilton RD, Walz JY. Synergistic effects of polymers and surfactants on depletion forces. Langmuir 2007;23:4351–7. http://dx.doi.org/10.1021/la063191d.
[12] Melby P, Prevost A, Egolf DA, Urbach JS. Depletion force in a bidisperse granular layer. Phys Rev E 2007;76:051307. http://dx.doi.org/10.1103/PhysRevE.76.051307.
[13] Lang PR. Depletion interaction mediated by polydisperse rods. J Chem Phys 2007;127:124906. http://dx.doi.org/10.1063/1.2775452.
[14] July C, Kleshchanok D, Lang PR. Shear-affected depletion interaction. Eur Phys J E Soft Matter 2012;35:60. http://dx.doi.org/10.1140/epje/i2012-12060-7.
[15] Lekkerkerker HNW, Tuinier R. Colloids and the depletion interaction. Berlin: Springer; 2011.
[16] Israelachvili JN. Intermolecular and surface forces. London: Academic Press; 2011.
[17] Nikolov AD, Kralchevsky PA, Ivanov IB, Wasan DT. Ordered micelle structuring in thin films formed from anionic surfactant solutions: II. Model development. J Colloid Interface Sci 1989;133:13–22. http://dx.doi.org/10.1016/0021-9797(89)90279-8.
[18] Kralchevsky PA, Denkov ND. Analytical expression for the oscillatory structural surface force. Chem Phys Lett 1995;240:385–92. http://dx.doi.org/10.1016/0009-2614(95)00539-G.
[19] Chu XL, Nikolov AD, Wasan DT. Thin liquid film structure and stability: the role of depletion and surface-induced structural forces. J Chem Phys 1995;103:6653–61. http://dx.doi.org/10.1063/1.470395.
[20] Nikolov AD, Wasan DT. Ordered micelle structuring in thin films formed from anionic surfactant solutions: I. Experimental. J Colloid Interface Sci 1989;133:1–12. http://dx.doi.org/10.1016/0021-9797(89)90278-6.
[21] Nikolov AD, Wasan DT, Denkov ND, Kralchevsky PA, Ivanov IB. Drainage of foam films in the presence of nonionic micelles. Prog Colloid Polym Sci 1990;82:87–98. http://dx.doi.org/10.1007/BFb0118245.
[22] Mitchell DJ, Ninham BW, Pailthorpe BA. Solvent structure in particle interactions. Part 2.—Forces at short range. J Chem Soc Faraday Trans 1978;2(74):1116–25.
[23] Horn RG, Israelachvili JN. Direct measurement of forces due to solvent structure. Chem Phys Lett 1980;71:192–4. http://dx.doi.org/10.1016/0009-2614(80)80144-8.
[24] Kjellander R, Sarman S. On the statistical mechanics of inhomogeneous fluids in narrow slits. An application to a hard-sphere fluid between hard walls. Chem Phys Lett 1988;149:102–8. http://dx.doi.org/10.1016/0009-2614(88)80357-9.
[25] Basheva ES, Kralchevsky PA, Danov KD, Ananthapadmanabhan KP, Lips A. The colloid structural forces as a tool for particle characterization and control of dispersion stability. Phys Chem Chem Phys 2007;9:5183–98. http://dx.doi.org/10.1039/B705758J.
[26] Zeng Y, Grandner S, Oliveira CLP, Thünemann AF, Paris O, Pedersen JS, et al. Effect of particle size and Debye length on order parameters of colloidal silica suspensions under confinement. Soft Matter 2011;7:10899–909. http://dx.doi.org/10.1039/c1sm05971h.
[27] Parker JL, Richetti P, Kékicheff P, Sarman S. Direct measurement of structural forces in a supermolecular fluid. Phys Rev Lett 1992;68:1955–8. http://dx.doi.org/10.1103/PhysRevLett.68.1955.
[28] Sheludko A. Thin liquid films. Adv Colloid Interface Sci 1967;1:391–464. http://dx.doi.org/10.1016/0001-8686(67)85001-2.

[29] Mysels KJ, Jones MN. Direct measurement of the variation of double-layer repulsion with distance. Discuss Faraday Soc 1966;42:42–50. http://dx.doi.org/10.1039/DF9664200042.
[30] Kralchevsky PA, Danov KD, Anachkov SE. Micellar solutions of ionic surfactants and their mixtures with nonionic surfactants: theoretical modeling vs. experiment. Colloid J 2014;76:255–70. http://dx.doi.org/10.1134/S1061933X14030065.
[31] Henderson D. An explicit expression for the solvent contribution to the force between colloidal particles using a hard sphere model. J Colloid Interface Sci 1988; 121:486–90. http://dx.doi.org/10.1016/0021-9797(88)90450-X.
[32] Attard P, Parker JL. Oscillatory solvation forces: a comparison of theory and experiment. J Phys Chem 1992;96:5086–93. http://dx.doi.org/10.1021/j100191a063.
[33] Pollard ML, Radke CJ. Density-functional modeling of structure and forces in thin micellar liquid films. J Chem Phys 1994;101:6979–91. http://dx.doi.org/10.1063/1.468325.
[34] Chu XL, Nikolov AD, Wasan DT. Monte Carlo simulation of inlayer structure formation in thin liquid films. Langmuir 1994;10:4403–8. http://dx.doi.org/10.1021/la00024a002.
[35] Blawzdziewicz J, Wajnryb E. Phase equilibria in stratified thin liquid films stabilized by colloidal particles. EPL-Europhys Lett 2005;71:269–75. http://dx.doi.org/10.1209/epl/i2004-10534-5.
[36] Trokhymchuk A, Henderson D, Nikolov A, Wasan DT. A simple calculation of structural and depletion forces for fluids/suspensions confined in a film. Langmuir 2001;17:4940–7. http://dx.doi.org/10.1021/la010047d.
[37] Christov NC, Danov KD, Zeng Y, Kralchevsky PA, von Klitzing R. Oscillatory structural forces due to nonionic surfactant micelles: data by colloidal-probe AFM vs. theory. Langmuir 2010;26:915–23. http://dx.doi.org/10.1021/la902397w.
[38] Carnahan NF, Starling KE. Equation of state for nonattracting rigid spheres. J Chem Phys 1969;51:635–6. http://dx.doi.org/10.1063/1.1672048.
[39] Reiss H, Frisch HL, Helfand E, Lebowitz JL. Aspects of the statistical thermodynamics of real fluids. J Chem Phys 1960;32:119–24. http://dx.doi.org/10.1063/1.1700883.
[40] Derjaguin BV. Untersuchungen über die Reibung und Adhäsion, IV (Analysis of friction and adhesion, IV). Kolloid Z (in German) 1934;69:155–64. http://dx.doi.org/10.1007/BF01433225.
[41] White LR. On the Deryaguin approximation for the interaction of macrobodies. J Colloid Interface Sci 1983;95:286–8. http://dx.doi.org/10.1016/0021-9797(83)90103-0.
[42] Derjaguin BV, Churaev NV, Muller VM. Surface forces. New York: Plenum Press, Consultants Bureau; 1987(Chapter 2).
[43] Kralchevsky PA, Nagayama K. Particles at fluid interfaces and membranes. Amsterdam: Elsevier; 2001[Chapter 5. http://store.elsevier.com/product.jsp?isbn=9780080538471].
[44] Rentsch S, Pericet-Camara R, Papastavrou G, Borkovec M. Probing the validity of the Derjaguin approximation for heterogeneous colloidal particles. Phys Chem Chem Phys 2006;8:2531–8. http://dx.doi.org/10.1039/B602145J.
[45] Ivanov IB, Toshev BV. Thermodynamics of thin liquid films. Colloid Polym Sci 1975; 253:593–9. http://dx.doi.org/10.1007/BF01753962.
[46] Alder BJ, Wainwright TE. Phase transition for a hard sphere system. J Chem Phys 1957;27:1208–9. http://dx.doi.org/10.1063/1.1743957.
[47] Anderson VJ, Lekkerkerker HNW. Insights into phase transition kinetics from colloid science. Nature 2002;416:811–5. http://dx.doi.org/10.1038/416811a.
[48] Borbély S. Aggregate structure in aqueous solutions of Brij-35 nonionic surfactant studied by small-angle neutron scattering. Langmuir 2000;16:5540–5. http://dx.doi.org/10.1021/la991265y.
[49] Danov KD, Basheva ES, Kralchevsky PA, Ananthapadmanabhan KP, Lips A. The metastable states of foam films containing electrically charged micelles or particles: experiment and quantitative interpretation. Adv Colloid Interface Sci 2011;168: 50–70. http://dx.doi.org/10.1016/j.cis.2011.03.006.
[50] Anachkov SE, Danov KD, Basheva ES, Kralchevsky PA, Ananthapadmanabhan KP. Determination of the aggregation number and charge of ionic surfactant micelles from the stepwise thinning of foam films. Adv Colloid Interface Sci 2012;183–184: 55–67. http://dx.doi.org/10.1016/j.cis.2012.08.003.
[51] Trokhymchuk A, Henderson D, Nikolov A, Wasan DT. Computer modeling of ionic micelle structuring in thin films. J Phys Chem B 2003;107:3927–37. http://dx.doi.org/10.1021/jp0210374.
[52] Henderson D, Trokhymchuk A, Nikolov A, Wasan DT. In-layer structuring of like-charged macroions in a thin film. Ind Eng Chem Res 2005;44:1175–80. http://dx.doi.org/10.1021/ie049714z.